11th International Workshop on Ship and Marine Hydrodynamics
Hamburg, Germany, September 22-25, 2019

Adaptive Path Tracking of the Underway Replenishment in Consideration of the Hydrodynamic Interactions between Two Ships

Yi Liu[1, 2], Zhihua Zeng[2], Zaojian Zou[2], Sheming Fan[1,*], Peiyuan Feng[1]

[1]Marine Design and Research Institute of China
1688 South Xizang Road, 200011 Shanghai, China
[2]School of Naval Architecture, Ocean and Civil Engineering, Shanghai Jiao Tong University
800 Dongchuan Road, 200240 Shanghai, China

*Corresponding author, fan_sm@maric.com.cn

ABSTRACT

Underway replenishment is a common way for ship supply at present, and the manual manipulation is the usual mode in the present, which would be greatly affected by the helmsman's experience. It is expected that the automatic control mode will become the main mode in the future. During the process of ship underway replenishment, interaction disturbances between two ships exist, which should be accounted for controller design. In this paper, the ship-to-ship hydrodynamic interactions are analyzed by using Computational Fluid Dynamics (CFD) method. The influences of transversal and longitudinal distance between two ships on the hydrodynamic interactions are illustrated. The details of the flow filed, such as pressure distributions on the two ship hulls and wave patterns are discussed to get a deeper insight into the physical flow mechanism during the underway replenishment. Then the ship motion model in consideration of the hydrodynamic interactions between two ships of underway replenishment is presented. The model predictive control (MPC) technology is adopted to control the yaw motion. To minimize the cross-track error and compensate for the drift effect caused by the hydrodynamic interactions between two ships, the integral line of sight (ILOS) guidance law is used for generating the desired heading angle. Finally, the computer simulations are conducted to evaluate the efficiency of the controller.

Keywords: Underway Replenishment; CFD; Ship-to-ship interactions; MPC; ILOS.

1 INTRODUCTION

When the ship is sailing on the sea, the food, fresh water and fuel are constantly consumed. In order to guarantee the normal operation of the ship, the consumed material need to be timely suppled. While the ship often cannot be always supplied near the port due to numerous factors, such as port capacity, the traffic of waterways or state of the sea, and the underway replenishment becomes a common way. During the underway replenishment, the supply ship is to maintain steady course and speed while the receiving ship moves up alongside the supply ship to receive the required material. The manual manipulation is the usual mode for the receiving ship to approach the supply ship, which would be greatly affected by the helmsman's skills or the conning officer of both ships. In addition, when the two ships start to operate in close proximity, their maneuvering behaviour becomes affected by the hydrodynamic interaction forces between them. These will greatly increase the risk of the operation during the underway replenishment. In this paper, adaptive control algorithms for path tracking during the underway replenishment are proposed in consideration of the hydrodynamic interactions between two ships, which can increase the efficiency and extend the operating conditions.

The interaction disturbances between two ships manoeuvring on close parallel courses are not completely understood so far, which trigger many experimental, theoretical, and numerical studies. Vantorre et al. [1] conducted a series of the model tests of ship-to-ship interactions for two ships in head-on encountering and overtaking operations, and practical semi-empirical formulae about the interaction

hydrodynamic forces on the two ships were promoted. Lataire et al. [2] conducted series of captive model tests for the ship lightering operation to improve the mathematical simulation models. Recently, Sano and Yasukawa [3] conducted the captive model tests for a front-back and left-right asymmetric ship and a mathematical model for the manoeuvring simulation were established to discuss the maneuverability of the combined two-ship unit. As for numerical approach, Yuan et al [4] estimated the hydrodynamic interaction effects in time domain by using three dimensional potential flow theory. Similarly, Xu et al. [5] developed a three-dimensional high-order panel method for predicting the ship-to-ship hydrodynamic interactions during meeting and overtaking in shallow water. Other than the potential theory based method, Zou et al. [6] presented numerical studies of the ship-to-ship interactions during a lightering operation by means of Reynolds Averaged Navier-Stokes (RANS) method. Arslan et al [7] numerically simulated the unsteady cross flow over two ship sections in close proximity by using Large Eddy Simulation (LES) turbulence model and compared the results with measurements. Kok et al. [8] studied the berthed ship-passing ship hydrodynamic interactions using RANS solver in both model scale and full scale, and found that the difference in the model-scale and full-scale interaction forces and moment predications were not significant.

With the development of advanced control theory, automatic control for the underway replenishment has a great application prospect. However, the interaction disturbances between two ships cause great difficulty in the controller design for ship motions control. Fu et al. [9] developed a coupled nonlinear two-ship tracking model for addressing hydrodynamic interaction disturbances of underway replenishment and used an inverse optimal adaptive controller that guarantees disturbance rejection to exogenous disturbances while maintaining a desired separation between the two vessels. Skejic et al [10] used Newman-Tuck theory to estimate interaction forces between two ships and employed automatic steering and speed control algorithms for both ships to achieve high-precision and collision-free underway replenishment. For the automatic control theory, Kyrkjebø et al. [11] developed a control law for rendezvous control of ships by using the synchronization techniques, only the position/attitude measurements were required for the controller. In realistic implementations, the control inputs are the rudder angle and propeller revolution. Thus, the constrains of the rudder/propeller rate/saturation should be considered during the controller design stage. From this point of view, the model predictive control (MPC) technique is appropriate since it can consider these constrains explicitly. Oh and Sun [12] presented the MPC method to deal with the input constraints, but they did not consider the external disturbances. Shen et al. [13] studied the trajectory tracking control problem of an autonomous underwater vehicle by using the Lyapunov based MPC control, and the simulation results showed an enhanced trajectory tracking performance.

From the previous studies, it can be seen that in the automatic control modelling of the interaction forces, most of the studies are based on the empirical formulae or the potential theory, which would bring some inaccuracy. The objective of this study is to investigate the viscous flow and the interaction hydrodynamic forces of two ships during underway replenishment by using URANS simulations, then establish the adaptive control algorithms for path tracking in consideration of the interaction forces.

2 MATHEMATICAL MODEL

2.1 COORDINATE SYSTEM

As shown in Figure 1, two right-hand coordinate systems are established to describe the ship motion on the horizontal plane: the earth-fixed coordinate system o_n-$x_n y_n$ and the body-fixed coordinate system o_b-$x_b y_b$. The o_n-$x_n y_n$ plane coincides with the still water surface, the x_n axis points to north, and the y_n points to south. The ship trajectories are described in the earth-fixed coordinate system. The body fixed coordinate system moves along with the ship hull, and the o_b-$x_b y_b$ plane coincides with the still water surface. Its origin is chosen at the centre of gravity of the ship. The x_b axis is in the mid-section of the ship, from the stern to the bow, and the y_b axis points to the starboard. The X, Y and N are the longitudinal force, transversal force and the yaw moment acting on the ship, respectively.

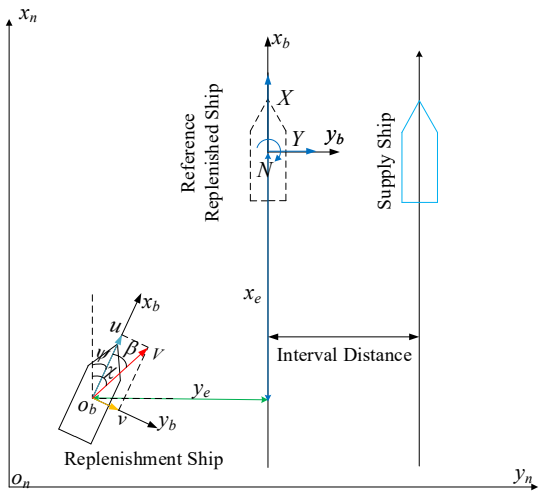

Figure 1: Coordinate systems and variables

2.2 SHIP MOTION MODEL CONSIDERING INTERACTION FORCES

The three degree-of-freedom ship motion in the horizontal plane is modelled using the MMG model (see Eq.(1)), in which the ship-to-ship interaction forces and moment are considered..

$$\begin{cases} (m+m_x)\dot{u}-(m+m_y)vr=-R(u)+X_{vv}vv+X_{vr}vr+X_{rr}rr+X_P(u,n)+X_R(\delta,u,v,r)+\tau^X_{\text{Interaction}} \\ (m+m_y)\dot{v}+(m+m_x)ur=Y_v v+Y_r r+Y_{vvv}vvv+Y_{vvr}vvr+Y_{vrr}vrr+Y_{rrr}rrr+Y_P(u,v,r)+Y_R(\delta,u,v,r)+\tau^Y_{\text{Interaction}} \\ (I_z+J_z)\dot{r}=N_v v+N_r(u)r+N_{vvv}vvv+N_{vvr}vvr+N_{vrr}vrr+N_{rrr}rrr+N_P(u,v,r)+N_R(\delta,u,v,r)+\tau^N_{\text{Interaction}} \end{cases} \quad (1)$$

where m and J are the mass and mass moment of inertia of the ship, m_x, m_y are the added mass in the directions of x axis and y axis, J_z is the added moment of inertia about z axis, R is the ship resistance, n is the propeller revolution, δ is the rudder angle; the subscripts "P" and "R" denote the force and moment components induced by propeller and rudder; X, Y, N with subscripts v or r are the hydrodynamic derivatives relating to v or r; $\left(\tau^X_{\text{Interaction}}, \tau^Y_{\text{Interaction}}, \tau^N_{\text{Interaction}}\right)$ are ship-to-ship interaction forces and moment, which are obtained by interpolating the simulation results of the CFD method.

2.3 MOTION CONTROL MODULE

2.3.1 MINIMIZATION OF THE CROSS-TRACK ERROR

The desired heading angle is generated by the adaptive ILOS guidance law [14],

$$\begin{cases} \psi_d = \gamma_p + \arctan\left(-\dfrac{y_e}{\Delta}-\hat{\beta}\right) \\ \dot{\hat{\beta}} = \kappa \exp\left(-|y_e|\right)\dfrac{U\Delta}{\sqrt{\Delta^2+\left(y_e+\Delta\hat{\beta}\right)^2}}y_e \quad \gamma>0 \end{cases} \quad (2)$$

where ψ_d is the desired heading angle; γ_p is the slope of the desired path; y_e is the cross track error; Δ is the lookahead distance, always equals to 4~5L; $\hat{\beta}$ is the estimated drift angle; $\kappa = 0.002$ is the adaptive gain.

The yaw dynamic is modelled by the Nomoto's first-order model,

$$T\ddot{\psi}+\dot{\psi}=K\delta+\xi \quad (3)$$

where the ξ represents the unmodelling dynamics and external disturbances.

The predicted heading angles by MPC are formulated as,

$$\boldsymbol{\psi}_p = \mathbf{F}\Delta\boldsymbol{\delta} + \mathbf{G}\boldsymbol{\psi}(k) \tag{4}$$

where $\boldsymbol{\psi}_p = \left[\psi(k+1|k), \psi(k+2|k)\ldots, \psi(k+N_p|k)\right]^{\mathrm{T}}$ is the predicted heading angles; $N_p = 8$ is the predicted horizon; $\Delta\boldsymbol{\delta} = \left[\Delta\delta(k), \Delta\delta(k+1), \ldots, \Delta\delta(k+N_c)\right]^{\mathrm{T}}$ is the current and future rudder angle increments; $N_c = 2$ is the control horizon; $\boldsymbol{\psi}(k) = \left[\psi(k), \psi(k-1)\right]^{\mathrm{T}}$ is the current and last heading angles; $\mathbf{F}$ and $\mathbf{G}$ are the solution of the Diophantine-Equation. The details can be found in [15].

Define the cost function as,

$$J = \left(\boldsymbol{\psi}_p - \boldsymbol{\psi}_d\right)^{\mathrm{T}} \boldsymbol{\Gamma}_1 \left(\boldsymbol{\psi}_p - \boldsymbol{\psi}_d\right) + \left(\Delta\boldsymbol{\delta}\right)^{\mathrm{T}} \boldsymbol{\Gamma}_2 \left(\Delta\boldsymbol{\delta}\right) \tag{5}$$

where $\boldsymbol{\psi}_d = \left[\psi_{d,k+1}, \ldots, \psi_{d,k+N_p}\right]$ is the desired heading angles, $\boldsymbol{\Gamma}_1$ and $\boldsymbol{\Gamma}_2$ are the weight matrices.

The limitation of rudder rate is formulated as,

$$\begin{aligned} \Delta\boldsymbol{\delta} &\le \Delta\delta_{\max} \\ \Delta\boldsymbol{\delta} &\ge -\Delta\delta_{\max} \end{aligned} \tag{6}$$

The future rudder angles and saturation of rudder are represented as,

$$\begin{aligned} \boldsymbol{\delta}_p &= \delta(k-1) + \begin{bmatrix} 1 & 0 & 0 \\ \vdots & \ddots & 0 \\ 1 & \cdots & 1 \end{bmatrix} \Delta\boldsymbol{\delta} \\ \boldsymbol{\delta}_p &\le \delta_{\max} \\ \boldsymbol{\delta}_p &\ge -\delta_{\max} \end{aligned} \tag{7}$$

Finally, the cost function and constrains compose a standard convex optimization problem. By solving this problem, the optimal control input can be obtained.

2.3.2 MINIMIZATION OF THE ALONG-TRACK ERROR

The desired surge velocity should be as large as possible when the along-track error is large, and when the along-track error is small, the desired surge velocity should close to the supply ship's surge velocity. Besides, the desired surge velocity should change smoothly. The following surge velocity guidance law proposed in this paper can achieve these objectives,

$$u_d = u_s\left(1 - \tanh(x_e / 3\mathrm{L})\right) + u_{\max}\tanh(x_e / 3\mathrm{L}) \tag{8}$$

where $u_s = 1.1\mathrm{m/s}$ is the surge velocity of the supply ship; x_e is the along-track error; $u_{\max} = 1.8\mathrm{m/s}$ is the maximum velocity of the receiving ship, corresponds to the propeller revolution equal to 700rpm.

The propeller revolution n_p can be obtained by the PID control,

$$n_p = k_p x_e + k_d\left(u_d - u_r\right) + k_i\int_0^t x_e dt + n_{p0} \tag{9}$$

where $k_p = 0.6, k_i = 0.001, k_d = 6$ is the tuneable parameters of the controller; a rectangular window is used for the integrator, in which the window length equals to 80; $n_{p0} = 538\mathrm{rpm}$ is the initial propeller revolution of the receiving ship.

3 NUMERICAL METHOD

The numerical study performed in the present work concerns the ship-to-ship interaction forces in calm and deep water. Since ONRT is one of the benchmark ships in ship hydrodynamics of CFD workshop2015 and SIMMAN2020, two different sizes of the ONR tumblehome (ONRT) hull forms without bilge keels, twin rudders and propellers are chosen,. The geometry of ONRT is shown in Figure 2, and its principal particulars are listed in Table 1. The scale ratios of the supply ship model and the receiving ship model are 34.96:1 and 48.94:1, respectively.

Figure 2: Geometry of the ONRT.

Table 1: Main particulars of ONRT

Particulars	**Full scale**	**Receiving Model （48.94:1）**	**Supply Model （34.96:1）**
Length L (m)	154.0	3.147	4.4058
Moulded breadth B (m)	18.78	0.384	0.5376
Draught T (m)	5.94	0.112	0.1568
DisplacementΔ (kg)	8.507×10^6	72.5	198.94
Block coefficient C_B (-)	0.535	0.535	0.535
Roll radius of gyration: k_x/L (-)	0.054	0.054	0.054
Pitch and yaw radiu of gyration: k_y/L, k_z/L (-)	0.250	0.246	0.246

The viscous flow around the hulls is assumed incompressible and is described by the RANS equations coupled with the time-averaged continuity equation. The CFD software STAR CCM+ is used to solve the equations. The RANS equations are closed by modelling the Reynolds stress tensor using the Shear Stress Transport (SST) k-ω turbulence model. A Finite Volume Method (FVM) is used to discretize the flow domain into a finite number of control volumes. Flow quantities near the wall are simulated according to an all y+ wall treatment by using a blended wall law to estimate shear stresses. The temporal discretization is based on a first-order Euler difference, and the spatial discretization is performed with second-order upwind scheme for the convection term and secondary gradient contribution for the diffusion term. The air-water interface is captured using the Volume of Fluid (VOF) method. The total amount of the computational domain grid is around 4×10^6. In order to attain the required accuracy and efficiently, multi-layer local refinements around the ships and near the free surface are carried out.

The computational domain and the corresponding boundary conditions are given in Figure 3. In the figure, $L_{\text{rec.}}$ is the length of the receiving ship model. Δx and Δy are the longitudinal and transverse distance between two hulls. Δx is defined as the distance between two mid-ships, while Δy is defined as the distance between the two ship centre-planes. Since in the practical operations, the relative distance between the receiving ship and supply ship is varied, three lateral distances have been selected: Δy =45, 52.5 and 60m in full scale; corresponding to Δy =0.29, 0.34 and $0.39L_{\text{rec.}}$ in model scale. A series of numerical simulations have been carried out at a wide range of longitudinal distances: Δx =±0.8, ±0.4, 0, -1.2, -1.8, and $-2.0L_{\text{rec.}}$ in model scale. The value of Δx is negative when the supply model is in the leading position, the value becomes positive when the receiving model overtakes the supply model. More cases of negative Δx are chosen because in most situations, the receiving ship catches up with the supply ship and then stays parallel with the supply ship. A nominal speed corresponding to $Fr = U/\sqrt{gL_{rec.}} = 0.2$ is selected for all numerical simulations.

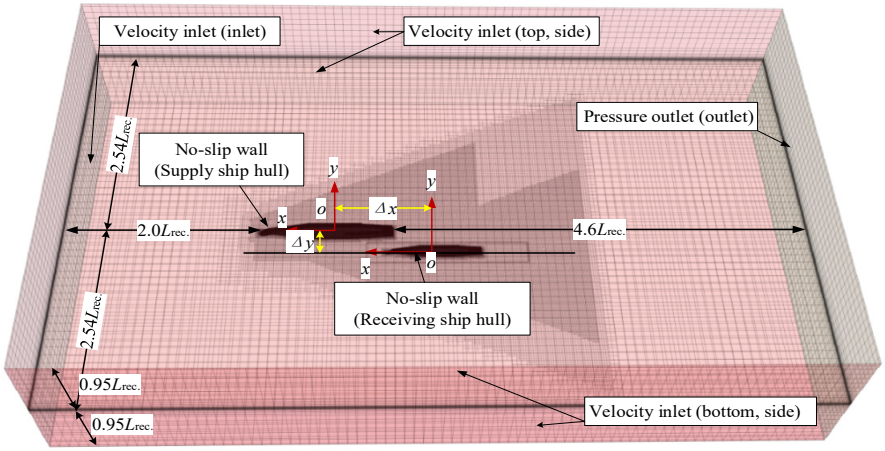

Figure 3: CFD computational domain and boundary conditions.

4 RESULTS AND DISSCUSSIONS

4.1 INTERACTION HYDRODYNAMIC FORCES

The computational hydrodynamic forces for the receiving ship model under different relative locations are given in Figure 4. The hydrodynamic forces are non-dimensionalized by:

$$X' = \frac{X}{0.5\rho U^2 L_{rec.}^2},\ Y' = \frac{Y}{0.5\rho U^2 L_{rec.}^2},\ N' = \frac{N}{0.5\rho U^2 L_{rec.}^3} \tag{10}$$

It can be seen in Figure 4 that the transversal and longitudinal separations have a great impact on the hydrodynamic forces on the ship. The trend of hydrodynamic forces of the receiving ship along with the longitudinal separations is generally the same at different transversal separations. If the receiving ship is slowly overtaking the supply ship, that is the process from $\Delta x/L_{rec.}$=-2.0 to $\Delta x/L_{rec.}$=0.8, the receiving ship's resistance decreases firstly and increases until $\Delta x/L_{rec.}$=-0.8, after which it increases and then reduces a bit again till the last position $\Delta x/L_{rec.}$=0.8, where the receiving ship is in front of the supply ship. As for the Y force, the receiving ship mostly encounters a negative transversal force when the receiving ship is far behind the supply ship ($\Delta x/L_{rec.}$<-0.5), indicating the force pushes the hull away. When the two mid-ships are close, the transversal force is behaved as attractive force. After that the Y force drops to negative. With respect to the yaw moment N', the yaw moments on the receiving ship is very small when the receiving ship is far behind the supply ship. If -0.8<$\Delta x/L_{rec}$<-0.4, that is to say, the receiving ship is located back of the supply ship, the yaw moment on the receiving ship is positive and increases, and then it decreases to the negative value with $\Delta x/L_{rec}$ varying from -0.4 to 0. When the receiving ship is in front of the supply ship, the absolute value of N decreases but still negative. It means that when the receiving ship is located back of the supply ship, the receiving ship turns towards the supply ship. While it is bow-away from the supply ship when the receiving ship is overtaking the supply ship.

For better understudying the ship-to-ship interactions, the wave pattern and the pressure distributions on the two hulls at different relative locations of two ships are given in Figures 5 and 6, respectively. It can be seen that the Kelvin envelope, divergence wave and transverse wave are greatly affected by position of the other ship. When the ship position is $\Delta x/L_{rec.}$=-0.8, $\Delta y/L_{rec.}$=0.29, divergence wave on the port side of the receiving ship is combined with the one of supply ship, while divergence wave on the starboard side is unapparent due to the interference of the supply ship; when the lateral distance becomes larger ($\Delta x/L_{rec.}$=-0.8, $\Delta y/L_{rec.}$=0.29), the divergence wave on the starboard side of the receiving ship is pronounced and the transverse wave trough increases. When the receiving ship is parallel to the supply ship ($\Delta x/ L_{rec}$ = 0.0), there is no divergence waves between the two ships. When the receiving ship is in front of the supply ship ($\Delta x/L_{rec.}$=0.8), the stern region of receiving ship is affected by the bow wave from the supply ship ($\Delta y/L_{rec.}$=0.29), while it becomes slightly when the lateral distance increases ($\Delta y/L_{rec.}$=0.39). The wave changes can also be reflected in the pressure distributions on the two hulls. As can be seen in Figure 6, the pressure distribution is asymmetric, which is greatly affect by the wave interference between the two ships.

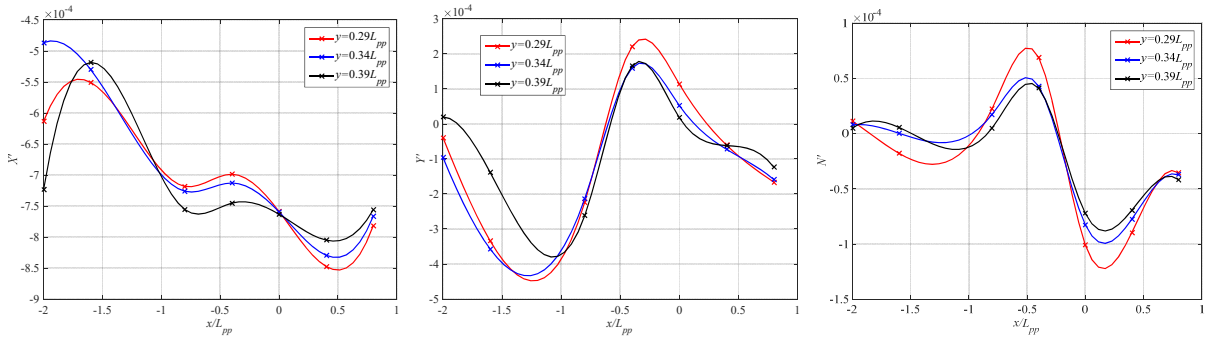

(a) X' (b) Y' (c) N'

Figure 4: The hydrodynamic forces and moment acting on the receiving ship at different relative locations of two ships.

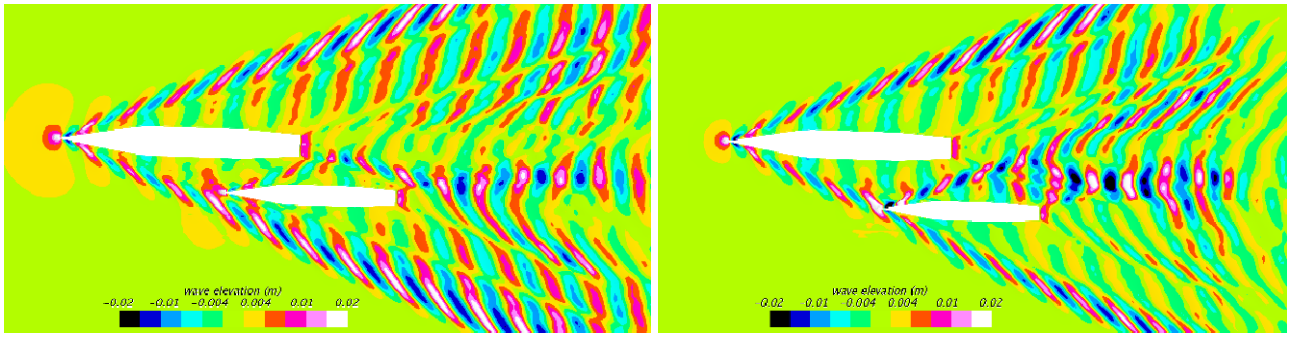

(a) $\Delta x/L_{\text{rec.}}$= -0.8, $\Delta y/L_{\text{rec.}}$=0.29 (b) $\Delta x/L_{\text{rec.}}$= -0.8, $\Delta y/L_{\text{rec.}}$=0.39

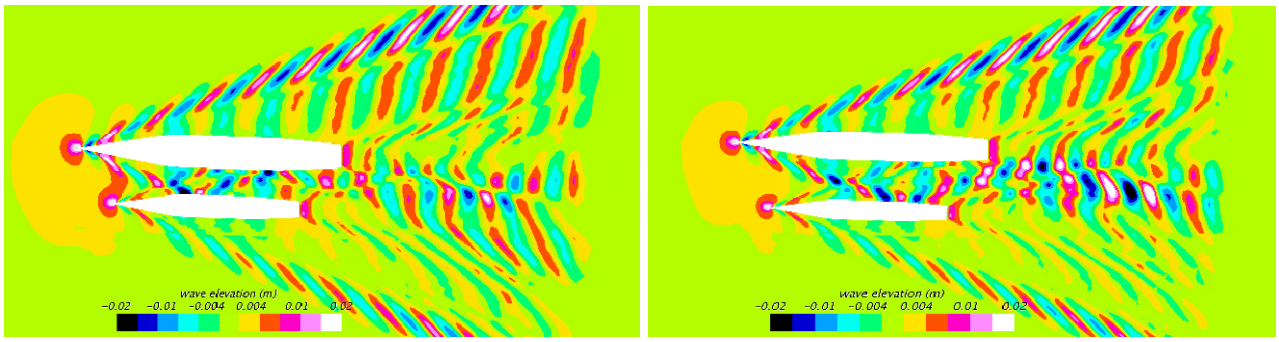

(c) $\Delta x/L_{\text{rec.}}$= 0.0, $\Delta y/L_{\text{rec.}}$=0.29 (d) $\Delta x/L_{\text{rec.}}$= 0.0, $\Delta y/L_{\text{rec.}}$=0.39

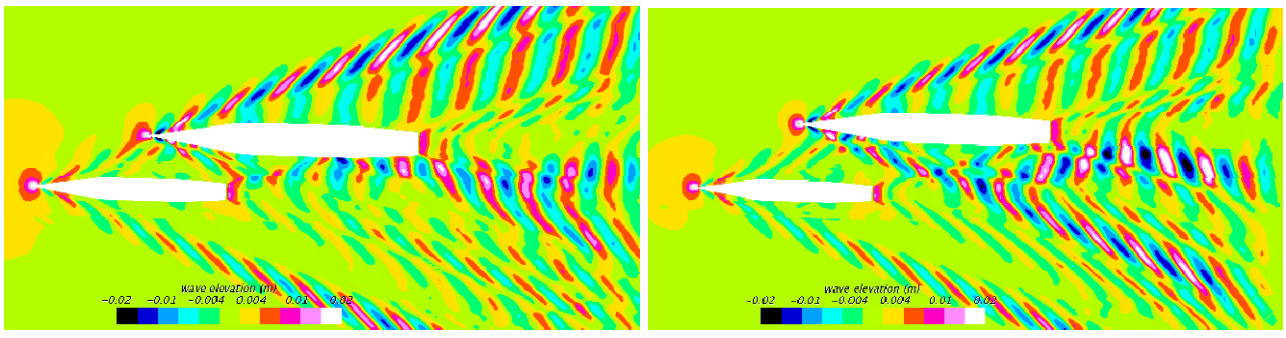

(e) $\Delta x/L_{\text{rec.}}$= 0.8, $\Delta y/L_{\text{rec.}}$=0.29 (f) $\Delta x/L_{\text{rec.}}$= 0.8, $\Delta y/L_{\text{rec.}}$=0.39

Figure 5: Wave pattern at different relative locations of two ships.

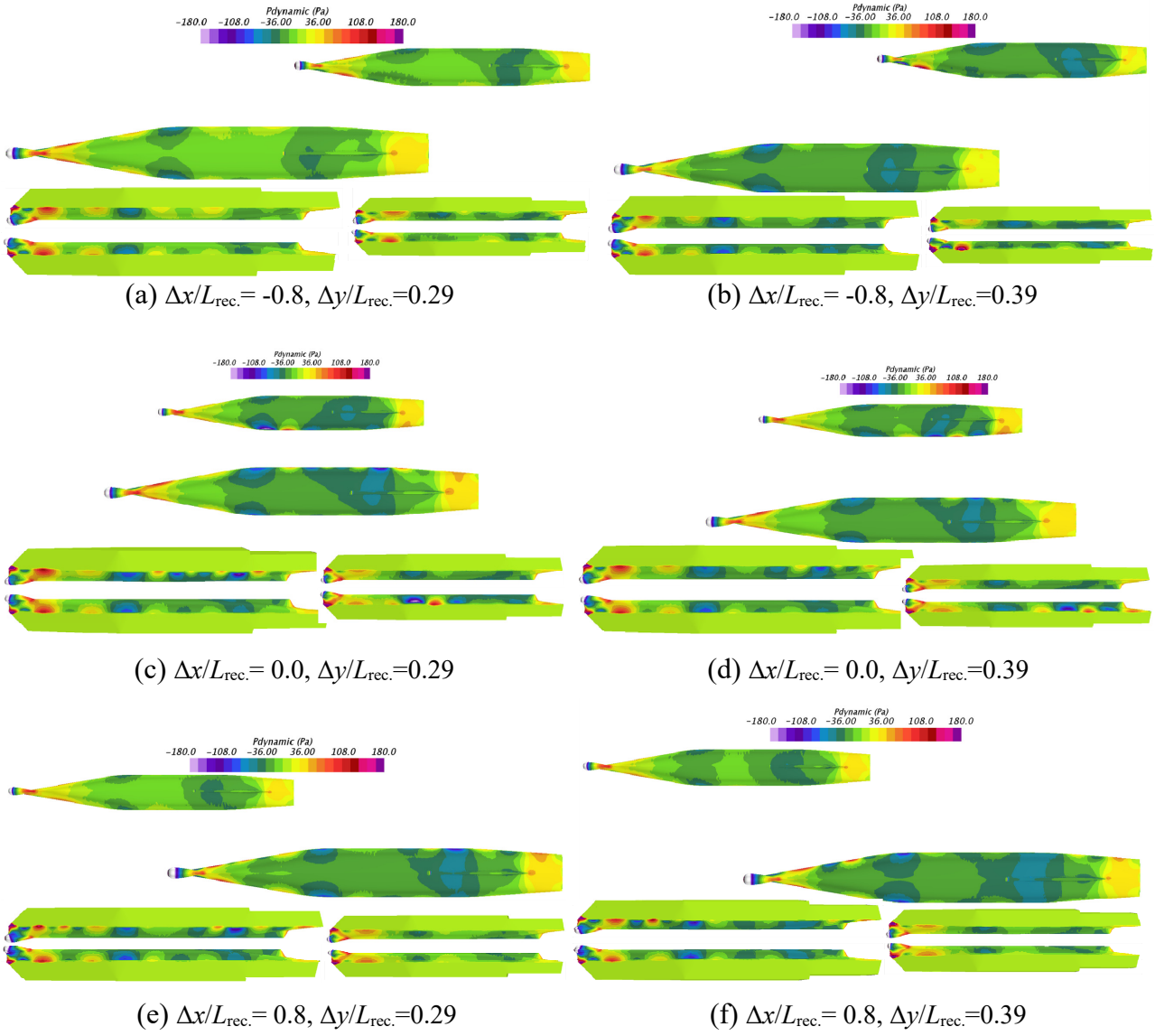

(a) $\Delta x/L_{rec.}$= -0.8, $\Delta y/L_{rec.}$=0.29

(b) $\Delta x/L_{rec.}$= -0.8, $\Delta y/L_{rec.}$=0.39

(c) $\Delta x/L_{rec.}$= 0.0, $\Delta y/L_{rec.}$=0.29

(d) $\Delta x/L_{rec.}$= 0.0, $\Delta y/L_{rec.}$=0.39

(e) $\Delta x/L_{rec.}$= 0.8, $\Delta y/L_{rec.}$=0.29

(f) $\Delta x/L_{rec.}$= 0.8, $\Delta y/L_{rec.}$=0.39

Figure 6: Pressure distributions at different relative locations of two ships.

4.2 SIMULATIONS BASED ON THE DESIGNED CONTROLLER

The supply ship is assumed moving straightforward with constant surge velocity in the present study, so only the receiving ship needs to be controlled. The yaw motion of the receiving ship is controlled by the MPC technology, while the surge motion is controlled by the guidance-based PID method. Computer simulations are conducted to evaluate the efficiency of the controller.

The initial position of the receiving ship is (-10m, 30m), the initial heading angle of the receiving ship is 30°, and the initial surge velocity of the receiving ship is the same as the supply ship. The supply ship is moving straightforward on the line y=0.32L_{rec} with constant surge velocity u_s=1.1m/s, the desired transversal distance is 0.32L_{rec}. Therefore, the receiving ship is expected to move alongside the supply ship on the line y=0. Firstly, the path tracking of the receiving ship is conducted without considering the ship-to-ship interaction forces. Figure 7(a) shows the corresponding time histories of heading angle and desired heading angle, rudder angle and propeller revolution. It can be seen that the heading angle can track the desired heading angle perfectly. Meanwhile, the rudder angle and propeller revolution satisfy the saturation and rate limitations. Figure 7(b) shows the estimated drift angle by the ILOS guidance law, the estimated drift angle converges to zero since the ship-to-ship interactions are neglected in this case. Figure 7(c) and 7(d) show the cross-track error and along-track error during the path tracking, it can be seen that these two errors converge to zero with small overshoot after about 100 seconds, which is useful in the realistic implements. Figure 8 shows the trajectories of the receiving ship and supply ship. The receiving ship moves fast in the initial phase

to chase after the supply ship. As the along-track error decreases, the surge velocity of the receiving ship closes to the surge velocity of the supply ship to avoid overshoot too much.

The path tracking simulation considering the ship-to-ship interaction forces is also conducted to investigate the influences on manoeuvring motion of the receiving ship. It can be seen from Figure 9(a) that the rudder angle fluctuates more serious when the receiving ship catches up with supply ship at about 50 seconds comparing to the case neglecting the interaction forces. Figure 9(b) shows the estimated drift angle during the path tracking. The estimated drift angle converges to a constant value after about 250 seconds. The receiving ship suffers a constant interaction forces (Figure 10) when it moves alongside the supply ship, so the drift angle is necessary for the receiving ship to counteract the sway force and yaw moment to keep sailing on the desired path. From Figure 9(c) and 9(d) the good path tracking performance can be observed.

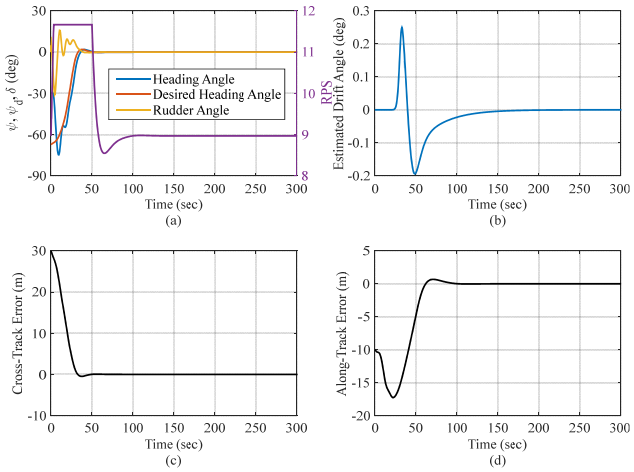

Figure 7: Path tracking without the interaction forces considered.

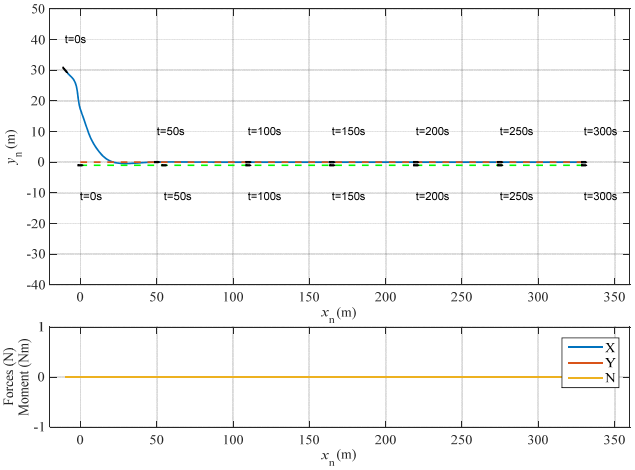

Figure 8: Trajectories of the receiving ship and the supply ship without the interaction forces considered.

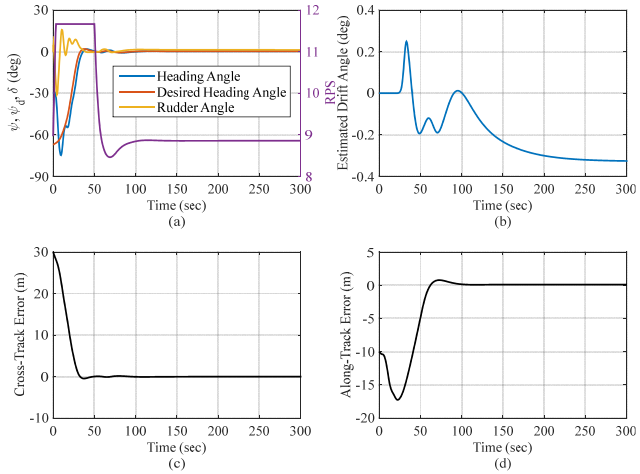

Figure 9: Path tracking with the interaction forces considered.

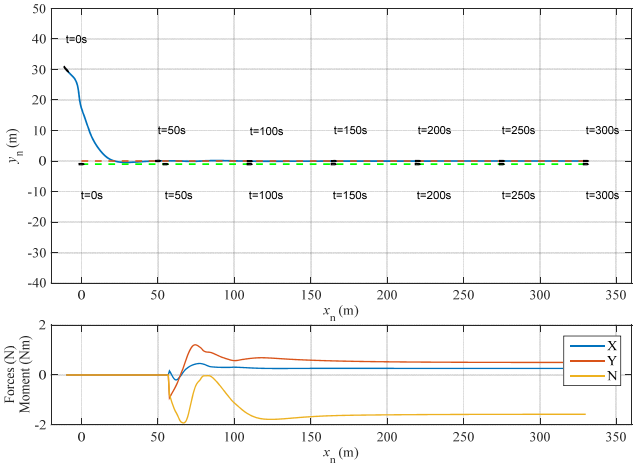

Figure 10: Trajectories of the receiving ship and the supply ship and the interaction forces on the receiving ship.

5 CONCLUSION

The present study investigates the viscous flow and the interaction hydrodynamic forces between two ONRT ship models during underway replenishment by using URANS simulations. The hydrodynamic forces of the received ship at different locations between two ships are presented. Moreover, with the advantages of CFD tools, more details of the flow field are also given to explain the hydrodynamic performance of the ships during underway replenishment. And the simulations reveal several influences of the ship-to-ship interactions such as relative positions and asymmetric ship wakes. An adaptive control algorithm for path tracking in consideration of the interaction forces is also established. Both the simulations with and without

considering the ship-to-ship interaction forces are conducted, and the simulation results prove the efficiency of the proposed controller.

In the future work, an experiment of the two ship models for underway replenishment will be performed in Marine Design and Research Institute of China (MARIC) to validate the presented mathematical model and numerical model. Moreover, the uncertainties about the CFD simulations will be conducted. The environment disturbances, such as waves and ocean currents will also be considered in the future work.

ACKNOWLEDGEMENTS

This work is financially supported by China Postdoctoral Science Foundation under Grant No. 2019M651596, to which the authors are most grateful.

REFERENCES

[1] Vantorre M., E. Verzhbitskaya, E. Laforce. “Model test based formulations of ship-ship interaction forces”. In: *Ship Technology Research*, 49(2002), 124-141.

[2] Lataire E., M. Vantorre, J. Vandenbroucke, et al. “Ship to ship interaction forces during lightering operations”. In: *2nd International conference on Ship Manoeuvring in Shallow and Confined Water: Ship to ship interaction*, Trondheim, Norway, 2011.

[3] Sano M., H. Yasukawa. “Maneuverability of a combined two-ship unit engaged in underway transfer”. In: *Ocean Engineering*, 173(2019), 774-793.

[4] Yuan Z. M., C. Y. Ji, A Incecik, et al. “Theoretical and numerical estimation of ship-to-ship hydrodynamic interaction effects”. In: *Ocean Engineering*, 121(2016), 239-253.

[5] Xu H. F., L Zou, Z. J. Zou, et al. “Numerical study on hydrodynamic interaction between two tankers in shallow water based on high-order panel method”. In: *European Journal of Mechanics-B/Fluids*, 74(2019), 139-151.

[6] Zou L., Z. J. Zou, Y. Liu. “CFD-based predictions of hydrodynamic forces in ship-tug boat interactions”. In: *Ships and Offshore Structures*, 2019 (published on line).

[7] Arslan T., J. Visscher, B. Pettersen, et al. “Numerical and experimental study of the flow around two ship sections side-by-side”. In: *33rd International Conference on Ocean, Offshore and Arctic Engineering*, San Francisco, United States, 2014.

[8] Kok Z., Y. Jin, S. Chai, et al. “URANS prediction of berthed ship–passing ship interactions”. In: *Ships and Offshore Structures*, 13(2018), 561-574.

[9] Fu S. H., C. C. Cheng, C. Y. Yin. “Nonlinear adaptive tracking control for underway replenishment process”, In: *IEEE International Conference on Networking, Sensing and Control,* 2004, Taipei, Taiwan, 2004.

[10] Skejic R., M. Breivik, T. I. Fossen, et al. “Modeling and control of underway replenishment operations in calm water”. In: *IFAC Proceedings Volumes*, 2009.

[11] Kyrkjebø E., K. Y. Pettersen. “Ship replenishment using synchronization control”. In: *IFAC Proceedings Volumes*, 2003.

[12] Oh S. R., J. Sun. “Path following of underactuated marine surface vessels using line-of-sight based model predictive control”. In: *Ocean Engineering*, 37(2010), 289-295.

[13] Shen C., Y. Shi, B. Buckham. “Trajectory Tracking Control of an Autonomous Underwater Vehicle Using Lyapunov-Based Model Predictive Control”. In: *IEEE Transactions on Industrial Electronics*, 65(2018), 5796-5805.

[14] Chen X., Z. Liu, J. Zhang, et al. “Path following of underactuated USV based on modified integral line-of-sight guidance strategies”. In: *Journal of Beijing University of Aeronautics & Astronautics*, 2018.

[15] Zeng Z. H., Z. H. Wang, J. Q. Wang, et al. “Path Following of Underactuated Marine Vehicles Based on Model Predictive Control”, In: *29th International Ocean and Polar Engineering Conference (ISOPE)*, Hawaii, USA, 2019.